Int. J. Multiphase Flow. Vol. 4, pp. 141–155. Pergamon/Elsevier. 1978. Printed in Great Britain

MEASUREMENT OF LOCAL SIZE AND VELOCITY PROBABILITY DENSITY DISTRIBUTIONS IN TWO-PHASE SUSPENSION FLOWS BY LASER-DOPPLER TECHNIQUE

S. L. LEE and J. SRINIVASAN
Department of Mechanical Engineering, State University of New York at Stony Brook, New York, U.S.A.

(*Received* 20 *March* 1977)

Abstract—A technique is presented for the simultaneous measurement of the local number and velocity probability densities of a dilute two-phase suspension which has a distribution of particle sizes and a predominate direction of flow orientation such as in the cases of pipe and boundary-layer flows. It is shown that by a suitable scheme of discrimination on the amplitude as well as the residence time and frequency of the individual Laser-Doppler bursts, one can obtain the statistics on the size number density distribution and, for each size range, velocity distribution of the particulate phase together with the velocity probability distribution of the fluid phase.

Results have been obtained for experiments conducted on a laminar uniform flow and a turbulent shear flow of a dilute glass particle–water suspension having a particle size distribution. Calibration needed for the scheme was accomplished by analyzing particle size and number density distribution data obtained from a Coulter particle sizing counter on a sample taken with an isokinetic probe.

INTRODUCTION

The application of Laser–Doppler anemometry in two-phase suspension flows presents considerable problems in obtaining statistics on such flow properties as particle size number density and velocity distributions. Consequently, most measurements using such a technique on two-phase suspensions are restricted to some rather simplified circumstances (Matthes *et al.* 1970; Golovin *et al.* 1971; Lee & Einav 1972; Einav & Lee 1973; Ben-Yosef *et al.* 1975; Durst & Zaré 1975; Mason & Birchenaugh 1975).

The problem on signal ambiguity concerns the oscillatory behavior of signal amplitude as a function of scattering angle and particle size in accordance with the Mie scattering theory. With fixed receiving optics, the signal amplitude still depends on the particle size in a complex way. Considerable effort has been devoted to the difficult task of precise sizing and velocity measurement of individual particles, by concentrating on particles of large enough size for the techniques of geometrical optics to be rendered useful (Durst & Zaré 1975), and by making use of an additional property of the signal (Farmer 1972; Durst & Eliasson 1975), for example. A careful evaluation of numerical computation of results of the amplitude function from Mie scattering theory reveals certain characteristics of the nature of these oscillations. For particles of moderately large sizes, they are found to be occuring in increasing frequency with increase in size and clustering around the nominal amplitude, which is increasing monotonically with size, in a confined manner. However, for a large class of problems of practical interest, such as the interpretations of the zodiacal light and of the light scattered from the Venus and Mars atmospheres, the interest is not centered on certain precise sizes but on some ranges of particle sizes. This amounts to an integration, over these size ranges, of the scattering from a cloud of particles with a given distribution of sizes. The qualitative effect is that the numerous maxima and minima shift in position with the size and the net result of the integration then is that these maxima and minima are washed out to a large extent (Van deHulst 1957). In addition, deviation of the actual conditions from conditions for the theory would further enhance this process. Therefore, in a suspension flow, if the selected width of the size window is narrow enough, the nominal or average amplitude of the signals can be expected to vary monotonically with the nominal or average size of the particles.

One additional serious problem on signal ambiguity originates from the inherent nonuni-

formity of illumination in the optical measuring volume (Farmer 1972). Some effort has been attempted to by-pass this difficulty, for instance, by incorporating a second optical system designed for particle sizing which is focused around the same probing point (Durst & Umhauer 1975). It still remains desirable to devise a scheme by which a central core region of the measuring volume where the illumination is more uniform, can be isolated out to serve as a new probing volume in the flow.

THEORY OF OPERATION

The operational arrangement of our reference-mode Laser–Doppler anemometer is shown in the sketch of figure 1. The oncoming laser beam from a 15 mW He–Ne CW Laser is split into two beams: the scatter beam which forms an angle of 7.5° with the transverse axis in a horizontal plane, and the reference beam. The measuring, scattering volume is approximately ellipsoidal, 250 μm in diameter and 800 μm in length. The receiving lenses are symmetrical with the sending lenses, and the scattering angle is fixed at nominally 15°. The received scattered beam from a moving scattering body passing through the scattering volume is brought to mix with an unshifted reference beam to generate a heterodyne on the photomultiplier tube surface to produce the Doppler frequency shift signal.

First, we assume that there is one particle in the measuring volume at a time. Because our measuring volume is so small, the maximum allowable number densities possibles to fulfill the requirement that we have one particle in the measuring volume at a time are quite large (up to about $10^5/cm^3$).

Secondly, we assume that the predominate direction of the flow coincides with the measuring direction of the Laser–Doppler anemometer system, which is the direction of bisecting line between the axes of the incident and receiving optics at the center of the measuring scattering volume. It is seen that the length of path of a particle passing through the measuring volume and the incident light intensity distribution along this path are essentially functions of the location of the path as sketched in figure 2. Since the particle path length is the product of signal path time and particle velocity which is directly proportional to the signal Doppler frequency, the three measurable characteristic parameters of a Doppler signal, as shown in figure 3, are then the amplitude, Doppler frequency and path time. In order to suppress the ambiguity on the particle size determination from a Doppler signal due to non-uniform distribution of incident light intensity inside the measuring volume, the effective measuring volume is electronically isolated to the central core portion of original measuring volume, in which the peak incident light intensity along any particle path falls within an arbitrarily small, pre-selected range.

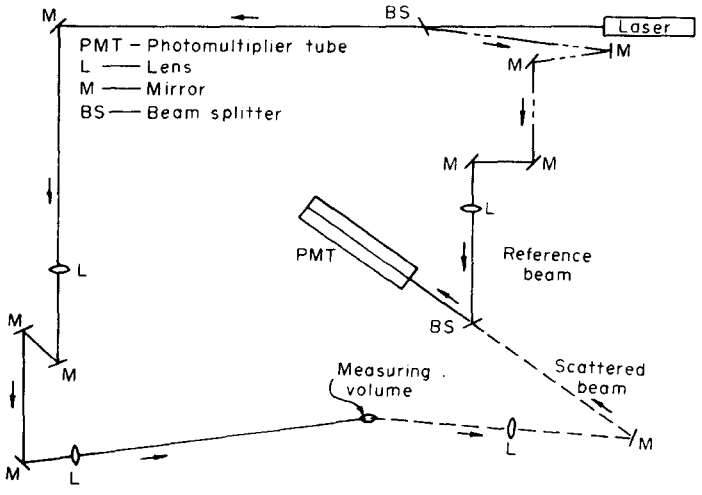

Figure 1. Optical arrangement.

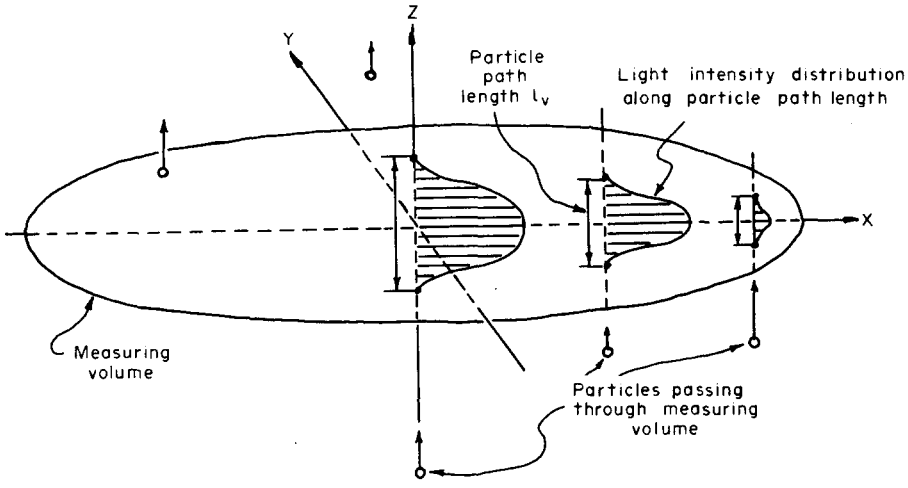

Figure 2. Sketch of optical measuring volume.

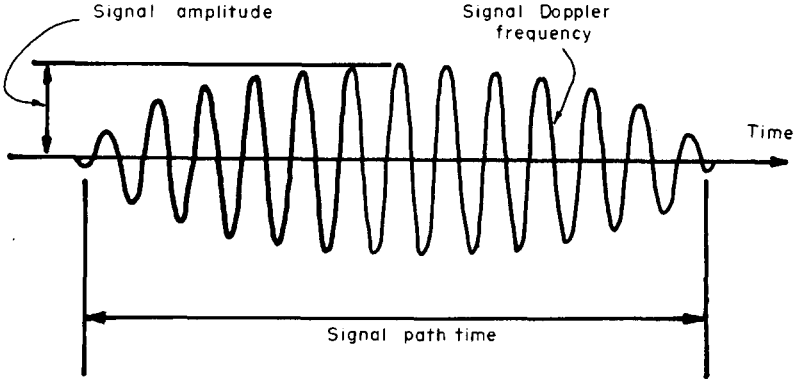

Figure 3. Sketch of particle Doppler signal.

Signal amplitude discrimination and isolated central core of measuring volume

Figure 4 gives a sketch of the dependence on path length l_v of the peak amplitude of signals from particles of a certain size d_i, as shown by curve (i), with the maximum peak amplitude A_i located along the maximum path length, l_m, passing through the center of the measuring volume. We will select a narrow amplitude discrimination window to operate on the signal peak amplitude, $\Delta A_i = (1-\delta)A_i$, such that $(1-\delta) \ll 1$, where δ is a constant close to unity. If all the particles are of exactly the same size d_i, the allowable signals are those from particles passing through the central core of the measuring volume, $\bar{l}_v < l_v < l_m$, where $\bar{l}_v$ is the limiting path length of this central core. However, when the particles have a distribution in size, the situation needs some clarification. In this case, the allowable signals in the central core region, as defined by signals from particles of size d_i, actually consist of, in varying proportions in the central core, signals from two adjacent particle size ranges, $d_{i'} \leqslant d \leqslant d_i$ and $d_i \leqslant d \leqslant d_{i''}$, being represented by curves (i') and (i'') respectively. For an extremely narrow amplitude window, say, for instance, $\Delta A_i = 0.05\, A_i$, the number density of particles within the affected size range can be considered statistically stable and the signals so discriminated should accurately represent those with a peak amplitude within the amplitude window ΔA_i around the nominal peak amplitude A_i.

The path length of a scattering particle through the measuring volume, l_v as shown in figure 5, can be determined from the product of the time of duration of the signal, τ, and the velocity of the particle, v_j, which is determined by the Doppler frequency of the signal itself, $l_v = \tau v_j$. By then ignoring all signals whose corresponding particle's path length is smaller than a chosen

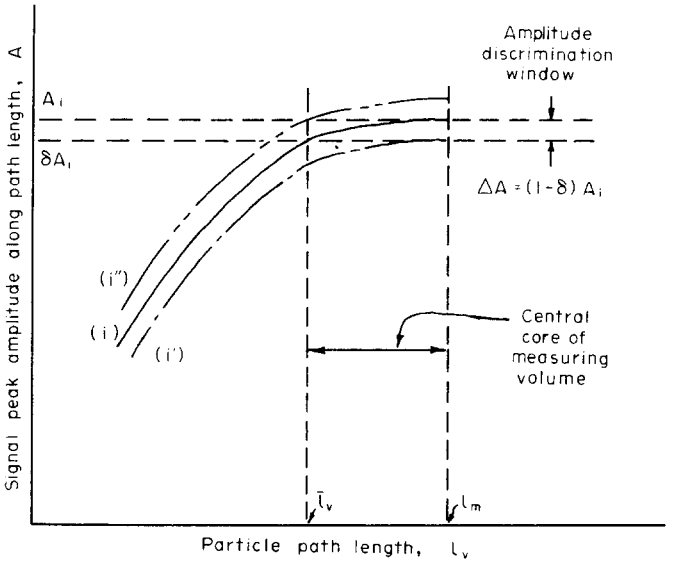

Figure 4. Sketch of signal amplitude discrimination scheme.

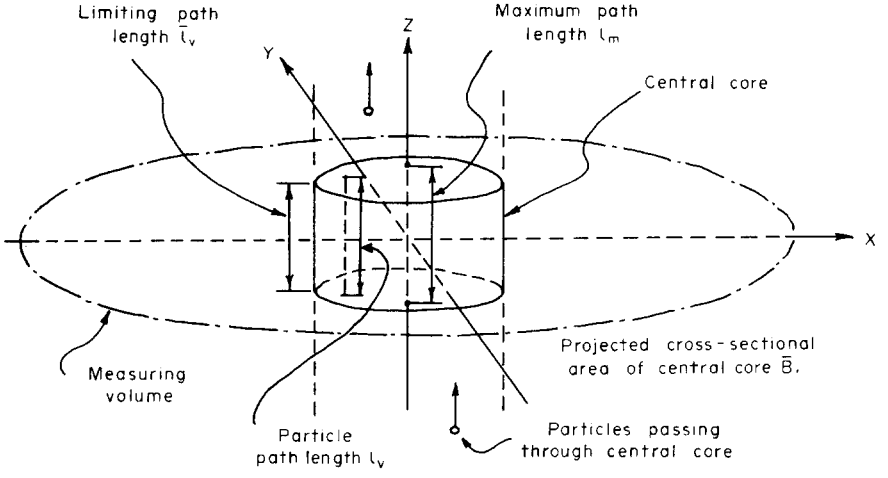

Figure 5. Sketch of electronically isolated central core of measuring volume.

lower limiting value $\bar{l}_v$, we can essentially eliminate the dependency of signal amplitude on particle position in the measuring volume. This is because the intensity of the incident light in the measuring volume is distributed approximately in a Gaussian manner, so that if only those particles passing through the central core region of the measuring volume ($\bar{l}_v \leq l_v \leq l_m$) are considered, the maximum amplitude of the Doppler signal envelope will then be dependent only on the particle size. The maximum path length, l_m (the one going through the geometrical center of the measuring volume) is obtained empirically, by determining the path lengths of many particles through calibration. The lower limiting volume of the path length for the central core, $\bar{l}_v$, is determined by the choice of a window size for the amplitude discrimination, which in turn is properly chosen from the range of distribution of amplitude of untreated Doppler signals from the particular flow under consideration.

Time and velocity discriminations

After signal amplitude discrimination, an additional discrimination on velocity will produce the required statistics on the particle size and velocity distributions. Unfortunately, the particle path time and velocity, rather than the particle path length, are readily obtainable from signals,

and a special scheme of combined time and velocity discrimination is needed to accomplish this goal.

Since the amplitude of the envolope of a Doppler signal varies in approximately a Gaussian fashion along a particle path through the measuring volume, the path length depends entirely on the base amplitude level, say A_τ. Because of the inherent noise level of the measuring system, the base amplitude level for path length or the equivalent path time determination is to be set a safe high enough level but still low enough for allowing even the low amplitude signals to be analyzed.

By setting a lower limit on the time duration τ, say $\bar{\tau}$, using a time discrimination scheme, and a related lower limit on the velocity v_j, $\bar{l}_v/\bar{\tau}$, using a velocity discrimination, we will retain signals within the velocity range $\bar{l}_v/\bar{\tau} \leq v_j \leq l_v/\bar{\tau}$ which can only be produced by particles going through the central core region of the measuring volume, $\bar{l}_v \leq l_v \leq l_m$, as shown by the sketch of figure 6.

However, this is not to say that these signals represent the signals produced by all the particles of the specified size d_i (corresponding to signal amplitude A_i) which pass through the central core region, because the signals from those particles which have a velocity above the upper limit of the local admissable velocity range, $l_v/\bar{\tau}$, that pass through the central core, will not be registered. It can be readily shown that the needed correction factor is

$$K = \frac{\text{Actual number count}}{\text{Correct number count}} = \int_0^{\bar{B}_0} \left[\frac{l_v - \bar{l}_v}{l_m - \bar{l}_v}\right] \frac{dB_0}{\bar{B}_0}$$

where $\bar{B}_0$ and B_0 are respectively the projected cross-sectional area of central core and the projected cross-sectional area bounded by contour of constant path length $l_v = l_v(B_0)$, a function of the geometry of the measuring volume. The value of $\bar{B}_0$ is determined from calibration with a flow of known number density $(N_i)_0$ and a uniform particle size d_i with the same velocity $(v_j)_0$ as shown in figure 7(a). The value of $(\dot{n}_{i,j})_0$, the probability density for this case, can be computed from the known number density $(N_i)_0$ and the measured velocity $(v_j)_0$, $(\dot{n}_{i,j})_0 = (N_i)_0(v_j)_0$. It should be noted that for this oversimplified case, $(\dot{n}_{i,j})_0$ simply stands for the number count of particles of size d_i having velocity $(v_j)_0$ per unit cross-sectional area of flow. By comparing this to the total number count for the whole central core region, obtained by a scheme of gradually raising the lower limit on the duration time discrimination, $\bar{\tau}$, the value of $\bar{B}_0$ can be obtained, since $\bar{B}_0$ is simply the ratio of this total number count to the number count per unit cross-sectional area of the central core, $(\dot{n}_{i,j})_0$. Here, $\bar{\tau}$ is gradually raised to such a critical value, say $\bar{\tau}_v$, that the number count n starts to decrease from the previously stable value $(n)_0$. This situation corresponds to the condition $\bar{l}_v/\bar{\tau}_v = (v_j)_0$ by which signals from all

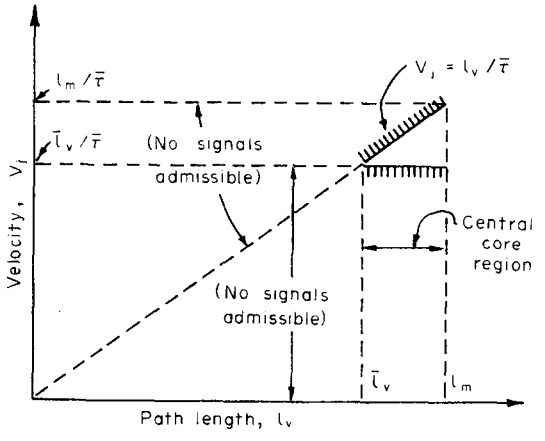

Figure 6. Sketch of criterion of signal admissibility due to duration time discrimination.

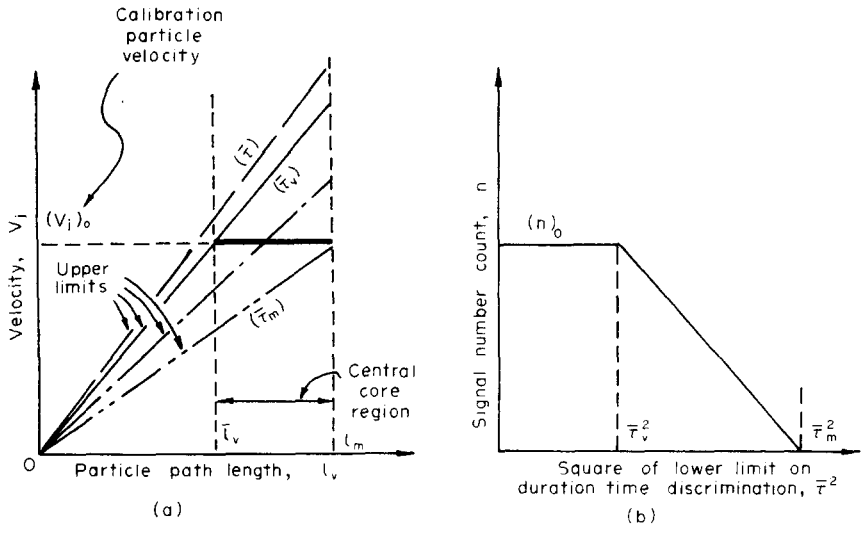

Figure 7. Sketch of calibration scheme.

particles passing through the central core region ($\bar{l}_v \leq l_v \leq l_m$) are registered, and the bounding path length for the central core, $\bar{l}_v$, is simply $\bar{\tau}_v(v_j)_0$ evaluated with the measured $(v_j)_0$ and the value of $\bar{\tau}_v$ so obtained. As $\bar{\tau}$ is finally raised to another critical value, say $\bar{\tau}_m$, the number count of signals becomes zero. This situation corresponds to the condition $l_m/\bar{\tau}_m = (v_j)_0$, and the maximum path length l_m (the one passing through the center of the measuring volume) is simply $\bar{\tau}_m(v_j)_0$ evaluated with the measured velocity $(v_j)_0$ and the value of $\bar{\tau}_m$ so obtained. To facilitate the determination of $\bar{\tau}_v$ and $\bar{\tau}_m$, the number count n is plotted against $(\bar{\tau})^2$ as suggested by an analysis of the path length through an ellipsoid. For a measuring volume approximately elliptical in shape, the plot should be made up of two approximately straight segments, as shown in figure 7(b).

It is of interest to note that since the number count n and the path length l_v, for this oversimplified case, are proportional respectively to B_0 and $\bar{\tau}$, the correction factor K, needed for converting the actual number count to corrected number count, can be readily obtained

$$K = \frac{1}{3}\frac{(2\bar{\tau}_m - \bar{\tau}_m\bar{\tau}_v - \bar{\tau}_v^2)}{(\bar{\tau}_m^2 - \bar{\tau}_v^2)}. \qquad [1]$$

The number count so corrected is then divided by the velocity range considered ($l_m/\bar{\tau} - \bar{l}_v/\bar{\tau}$) and size range Δd_i and the cross-sectional area of the central core ($\bar{B}_0$), to give the probability density $\dot{n}_{i,j}$, which is the number count per unit time per unit cross-sectional flow area, per unit velocity range and unit size range, for particles of size d_i and velocity v_j where v_j is now the mean velocity in the small velocity range considered (i.e. $v_j = (l_m/\bar{\tau} + \bar{l}_v/\bar{\tau})/2$).

Let $N_{i,j}$ = No. of particles of size d_i per unit volume, per unit velocity range and unit size range with the center velocity v_j.

Then

$$\dot{n}_{i,j} = N_{i,j}v_j \qquad [2]$$

and

$$N_i = \sum_j N_{i,j} = \sum_j \frac{\dot{n}_{i,j}}{v_j} \qquad [3]$$

where N_i = number density of particles of size d_i.

INSTRUMENTION AND EXPERIMENTAL APPARATUS

Instead of measuring the amplitude (A_i), time duration (τ) and velocity (v_j) of each signal, the output of the LDA is filtered as shown in figure 8. After an amplitude discrimination set on signal amplitude A_i and a time discrimination set on the lower limit on the signal path duration time $\bar{\tau}$, only the signals having an amplitude within the pre-selected narrow amplitude window in the neighborhood of A_i and a duration time $\tau \geqslant \bar{\tau}$ can reach the tracker. The tracker then converts the Doppler frequency of the signals into voltage signals proportional to the particle velocities. The output of the tracker is passed to a velocity discriminator circuit which allows through only those signals with a velocity about a value $\bar{l}_v/\bar{\tau}$. This results in signals for which the product $v_j \cdot \tau = l_v$ has a value greater than $\bar{l}_v$, and hence only for those particles passing through the central core region. The number count of such signals is executed on an electronic counter to give the measured number count of particles of a particular size and a particular velocity as previously described. By changing the time discriminator lower limit $\bar{\tau}$ and the corresponding velocity discriminator lower limit $\bar{l}_v/\bar{\tau}$, number counts at different velocities can be obtained for particles of the same size range. Then, by systematically changing the setting of the amplitude discriminator and repeating the aforementioned time and velocity discrimination schemes, statistics for the complete particle size range can be readily accomplished. Furthermore, by analyzing signals from particles of small enough size, the velocity probability distribution for the fluid phase can also be obtained, using these small particles as tracers. An instrumentation block diagram is shown in figure 9.

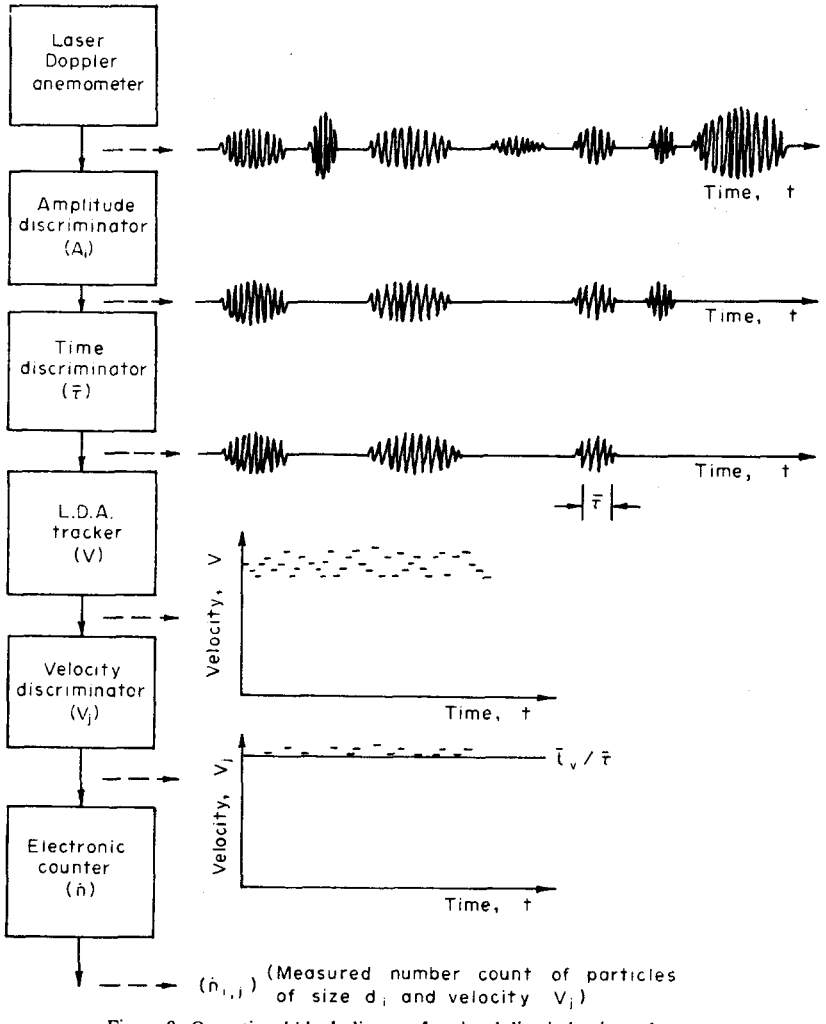

Figure 8. Operational block diagram for signal discrimination scheme.

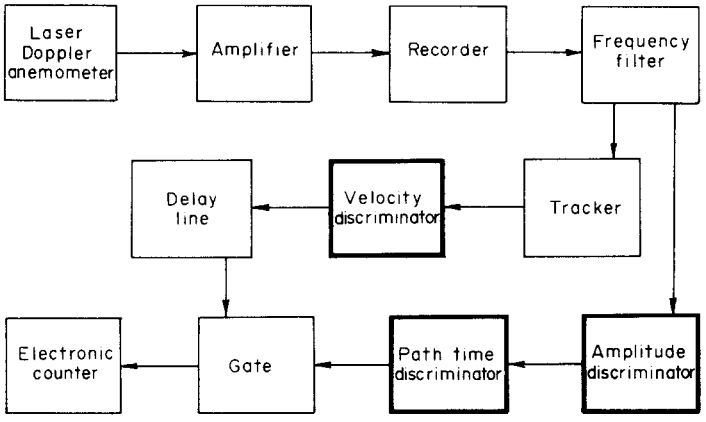

Figure 9. Instrumentation block diagram.

The flow apparatus consists mainly of a precision closed-loop water channel which has an effective length of 6.10 m and inside dimensions of 45.7 cm wide and 30.5 cm deep with walls made of optical grade plate glass. The entire optical system is mounted on top of a heavy traversing base, matching and aligned with the water channel, which is capable of positioning the optical measuring volume inside the water channel accurate to 25 μm in all three directions. The water channel receives its water supply from a Micronite filter with a maximum port size of 2 μm. Precision neutrally buoyant hollow glass spheres of sizes in a distributed range of up to 35 μm are added to the channel water loop to serve as the suspended phase. The Doppler signals from the optical anemometry system are first recorded on magnetic tape which is afterwards played back at a slower speed for data procession in the instrumentation system.

CALIBRATION

According to the calibration scheme as shown in figure 7, particles of one single precise size are needed, a feat not easily attainable because of the difficulty of obtaining such particles. A substitute way has been found in experimenting with very dilute suspension of particles of distributed sizes.

The optical measuring volume was placed in that portion of the water channel where a laminar uniform free stream flow, $(v_j)_0 = 6.43$ cm/s, was established as shown in figure 10. In a preliminary trial run, the amplitude discrimination window was deliberately made very narrow to scan over the whole amplitude range to obtain a rough picture of the signal amplitude distribution pattern. Due to the dilution of particles and the very narrow amplitude window size used, the signal amplitude displayed a near discrete size distribution at a very few isolated amplitudes. Any of these amplitudes could be tested for suitability as a substitute for one single precise size particle needed for calibration. One of them, $A_i = 770 \sim 810$ mV was finally adopted and its suitability for this task is demonstrated in the well behaved calibration curve of signal number count, n, vs square of lower limit on duration time, $\bar{\tau}^2$, as shown in figure 11. The duration time $\bar{\tau}$, based on tape speed of 38 cm/s, is twice as large as $\bar{\tau}$, based on the recording speed of 76 cm/s, and the operational amplitude window size $\Delta A_i = 0.05 A_i$. The total tape length is 200 m. The two important quantities characterizing the central core of the measuring volume for this case are found to be:

$$\bar{l}_v = 228\ \mu\text{m};$$

$$l_m = 267\ \mu\text{m}.$$

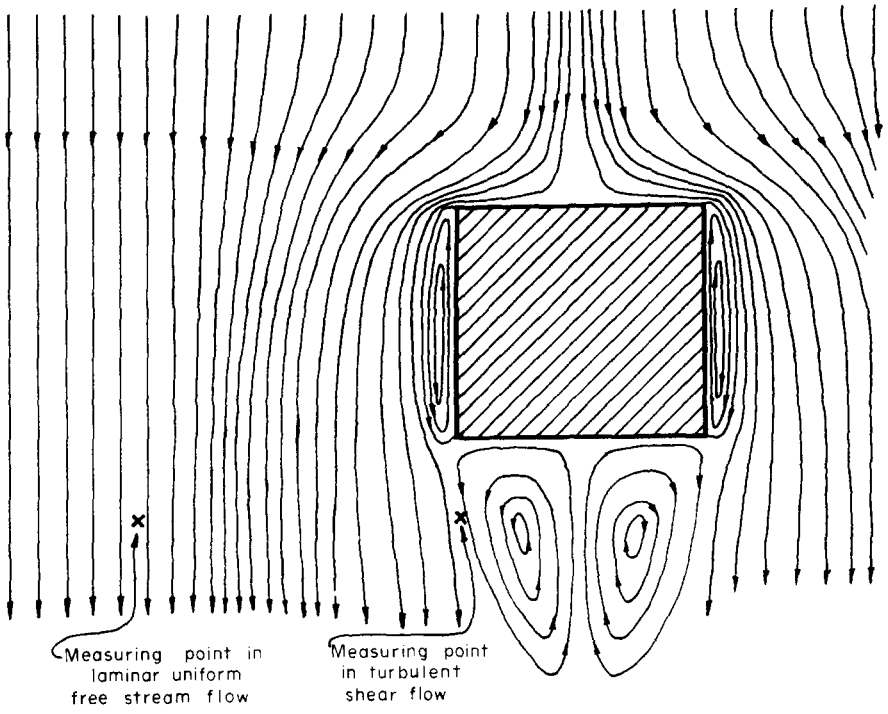

Figure 10. Flow of a two-phase suspension around a transverse rectangular body.

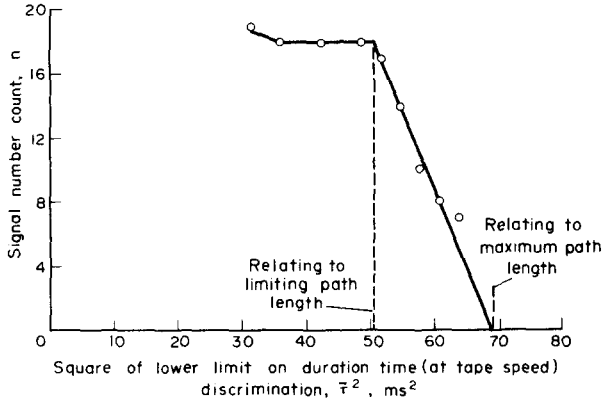

Figure 11. Calibration scheme for determination of limiting and maximum particle path length in central core of measuring volume.

And the correction factor needed for converting the actual number count to corrected number count, according to [1], has the value:

$$K = 0.536$$

The next step is to establish a calibration between the signal amplitude and particle size from the signal number count and particle number density from independent measurement of the water sample. The accumulative actual signal number count, $[n]$, for signals of amplitude from A_i to A_{max}, the maximum amplitude, for the various signal amplitudes is plotted in figure 12. The curve gives the limiting value:

$$[n] = 1, \quad \text{at} \quad A_{max} = 1.08\ \text{V}.$$

A water sample taken immediately downstream of the measuring volume with an isokinetic

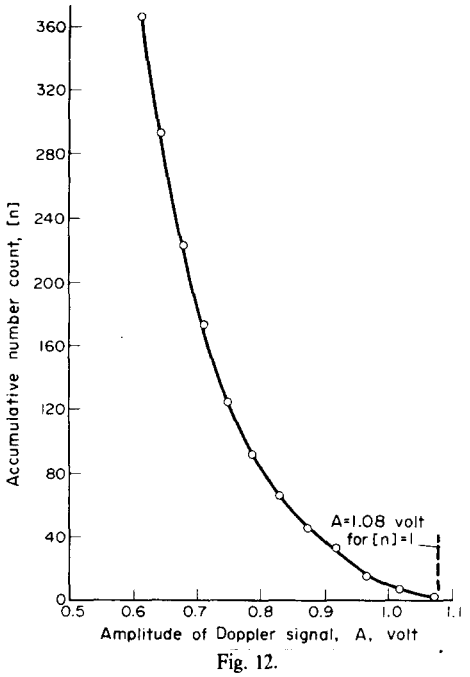

Fig. 12.

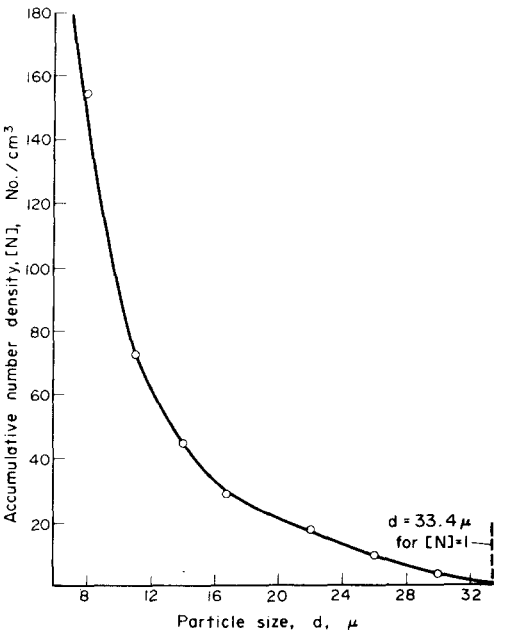

Fig. 13.

Figure 12. Signal amplitude and number count distribution.

Figure 13. Particle size and number density distribution obtained from counter sizing of mixture sample.

probe was analyzed with a Coulter (Model B) counter. The resulting accumulative particle number density count, $[N]$, for particles of size from d_i to $d_{\max}$, the maximum size, for the various particles sizes is plotted in figure 13. The curve gives the limiting value:

$$[N] = 1, \quad \text{at} \quad d_{\max} = 33.4\,\mu\text{m}.$$

By definition, we have for the uniform flow,

$$n_i = KN_i(v_j)_0\bar{B}_0T_0 = kN_i$$

where n_i = actual signal number count of signals of amplitude A_i; K = correction factor for signal number count; N_i = number density of particles of size d_i; $(v_j)_0$ = uniform mixture velocity; $\bar{B}_0$ = base cross-sectional area of central core of measuring volume; T_0 = tape recording time; $k = K(v_j)_0\bar{B}_0T_0$, a constant.
Therefore, we have the relationship

$$[n] = k[N]$$

between the two accumulative quantities. Furthermore, if we let

$$A^* = A_i/A_{\max} \quad \text{and} \quad d^* = d_i/d_{\max}$$

the following relations can be established:

$$\frac{\mathrm{d}\{\ln[N]\}}{\mathrm{d}(d^*)} = \frac{\mathrm{d}\{\ln[N]\}}{\mathrm{d}(A^*)}\frac{\mathrm{d}(A^*)}{\mathrm{d}(d^*)}$$

$$\frac{\mathrm{d}\{\ln[N]\}}{\mathrm{d}(A^*)} = \frac{1}{[N]}\frac{\mathrm{d}[N]}{\mathrm{d}(A^*)} = \frac{k}{[n]}\frac{1}{k}\frac{\mathrm{d}[n]}{\mathrm{d}(A^*)} = \frac{\mathrm{d}\{\ln[n]\}}{\mathrm{d}(A^*)}.$$

Therefore, we have

$$\frac{d\{\ln[N]\}}{d(d^*)} = \frac{d\{\ln[n]\}}{d(A^*)} \frac{d(A^*)}{d(d^*)}$$

which, after integration, becomes

$$\{\ln[N]\}|_{d^*}^{d^*=1} = \{\ln[n]\}|_{A^*}^{A^*=1}.$$

Since at $d^* = 1$: $N = 1$ and $\ln[N] = 0$ and at $A^* = 1$: $n = 1$ and $\ln[n] = 0$, we have

$$\ln[N]|_{\text{at } d^*} = \ln[n]|_{\text{at } A^*}.$$

which establishes a unique correlation relationship between d^* and A^* as shown by computational scheme of figure 14. The resultant calibration curve between the normalized particle size d^* and signal amplitude is shown in figure 15. Results from direct amplitude measurement using particles of five precise size ranges are also plotted for comparison. The dimensional calibration curve between particle size and signal amplitude is plotted in figure 16. Using this calibration, the resultant particle size and number density distribution in this laminar uniform free stream flow is plotted in figure 17.

Further, for the previous calibration run for the determination of $\bar{l}_v$, l_m and K as shown in figure 11, we have

$$(n)_0 = (N_i)_0 (v_j)_0 \bar{B}_0 T_0$$

where $(n)_0 = 18$, the stabilized number count; $(N_i)_0 = 20/\text{cm}^3$, the number density of particles of sizes between 10.5 μm and 12.5 μm, corresponding to amplitudes of 770 mV and 810 mV respectively, through the calibration curve, figure 16, at $13/\text{cm}^3$—μm from the number density

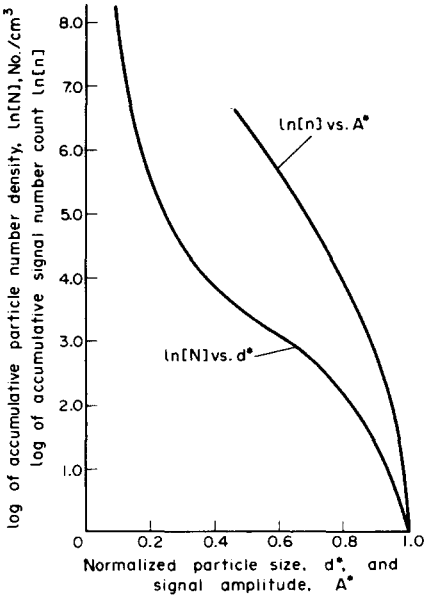

Fig. 14.

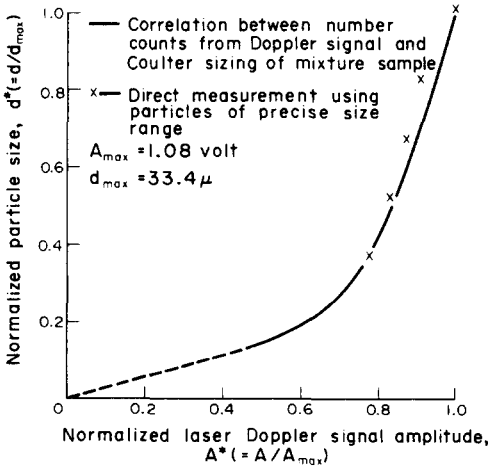

Fig. 15.

Figure 14. Correlation scheme used to obtain relationship between particle size and signal amplitude.

Figure 15. Comparison of signal amplitude calibration results from number count correlation and direct measurement using particles of precise size range.

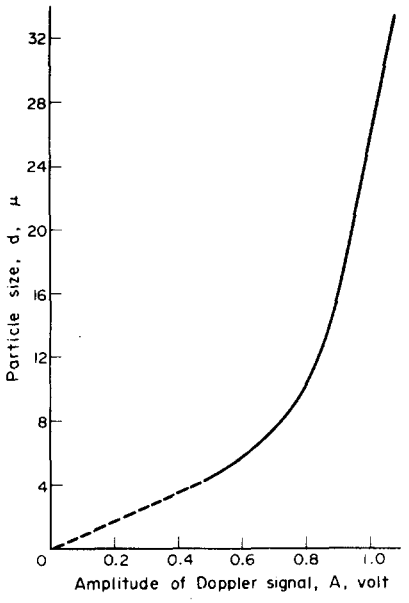

Fig. 16.

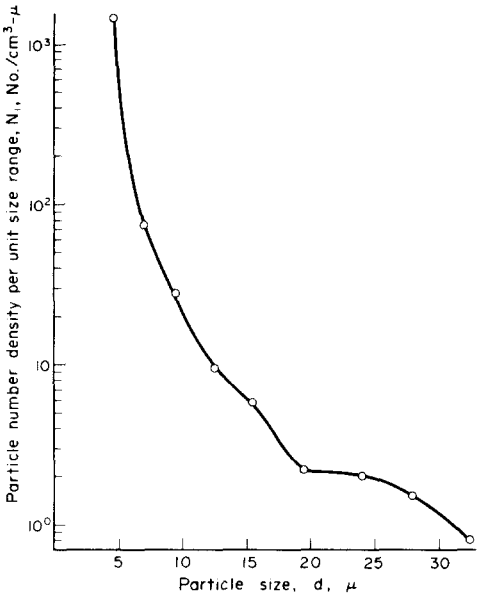

Fig. 17.

Figure 16. Calibration curve obtained from correlation between number counts from Doppler signal and counter sizing of mixture sample.

Figure 17. Particle size and number density distribution in laminar uniform flow.

distribution curve, figure 17; $(v_j)_0 = 6.43$ cm/s, the uniform free stream velocity; $T_0 = 484$ s, the tape recording time, and therefore, the base cross-sectional area of central core of measuring volume is then:

$$\bar{B}_0 = 4.44 \times 10^4 \, \mu\text{m}^2.$$

MEASUREMENT IN TURBULENT SHEAR FLOW

A measuring point was selected in a turbulent shear flow on the edge of the wake behind a transverse rectangular body, as shown in figure 10, where significant particulate accumulations and sizable velocity fluctuations are expected. The particle number counting rate per unit cross-sectional area per unit velocity range and unit size range was obtained from a length of tape of 110 m recorded at 76 cm/s for a total of 16 selected nominal particle sizes ranging from 4.45 μm to 32.5 μm. A three-dimensional plot of these results are shown in figure 18, exposing many interesting fine structural details.

Summing up the number density computed from each of the velocity ranges of the same nominal particle size, we obtain the particle number densities per unit size range for each of the 16 nominal particle sizes as shown by the plot of figure 19. For comparison purposes, the ratio of the particle number densities for a measuring point in a turbulent shear flow to the particle number density for a measuring point in the uniform laminar free stream flow for each of the 16 selected nominal particle sizes is plotted in figure 20. First, it is of interest to note that there is an order of magnitude increase in particulate content for all particle sizes in this turbulent shear flow over the ambient free stream flow apparently due to the enormous accumulation of particulates in the stagnation point flow on the upstream side of the rectangular transverse body, which is dumped into the neighboring regions downstream. Secondly, the fine structure of this distribution curve seems to bear evidence to the results of dynamic interactions experienced by the particles in so complex a flow as the present one. Thirdly, at the smaller size end, this distribution curve drops rapidly toward a value of unity at a particle size slightly under 4 μm. This point is quite significant in that the number density for the turbulent shear flow remains

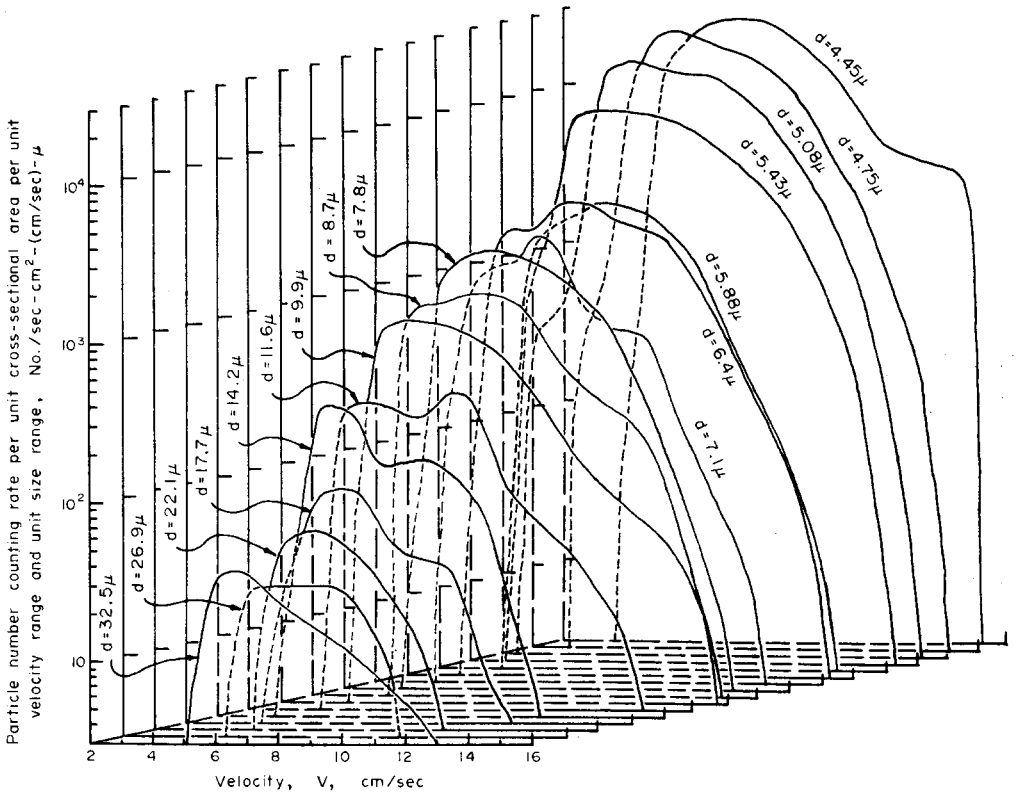

Figure 18. Sample particle size and velocity distribution in a turbulent shear flow of a suspension.

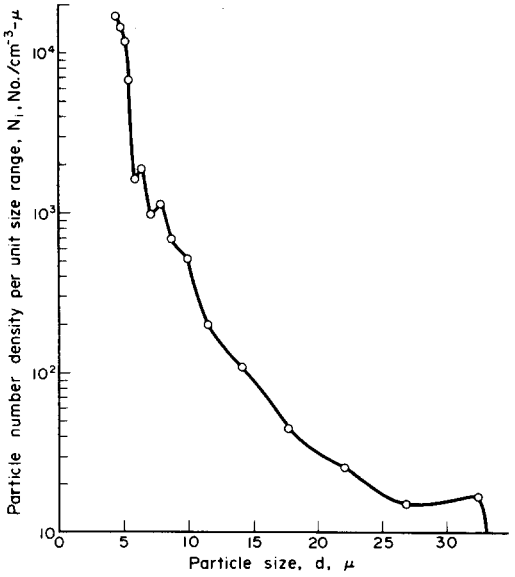

Figure 19. Sample particle size and number density distribution in a turbulent shear flow of a suspension.

the same as that of the free stream flow for particles smaller than slightly under 4 μm. The implication is then that such particles will closely follow the fluid motion and consequently can be used as tracers for fluid phase velocity measurement.

A segment of tape of 4.5 m length was analyzed in this light, using an amplitude discrimination scheme of blocking out signals with amplitudes larger than a selected small value. Results of the fluid phase velocity probability distribution in a turbulent shear flow are plotted using particles below 4.0 μ and 3.7 μ respectively as tracers for the fluid as shown in figure 21.

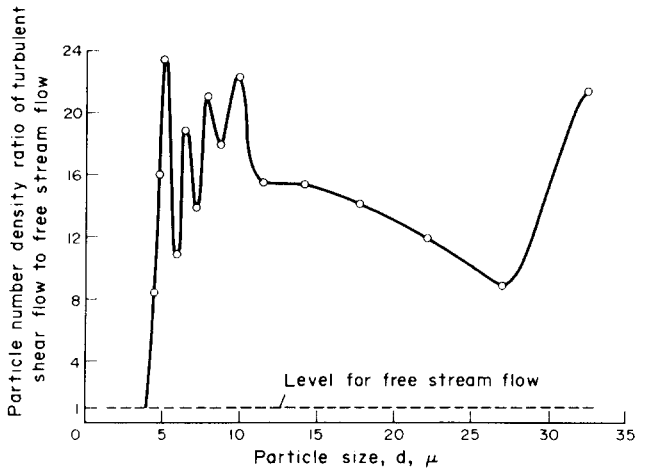

Figure 20. Distribution of particle number density ratio of turbulent shear flow to free stream flow.

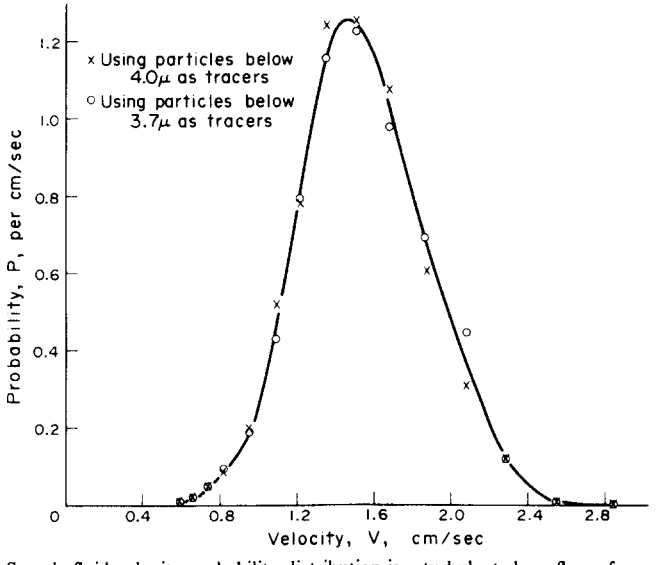

Figure 21. Sample fluid velocity probability distribution is a turbulent shear flow of a suspension.

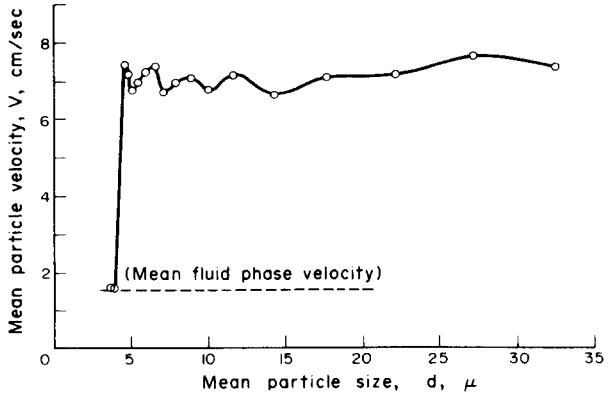

Figure 22. Distribution of mean particle velocity in a turbulent shear flow of a suspension.

A plot of the mean particle velocity as a function of mean particle size in this turbulent shear flow of a suspension is shown in figure 22.

CONCLUSION

A new experimental scheme has been developed for the measurement of the local number densities and velocity probability densities of a dilute two-phase suspension which has a distribution of particle size and a predominate direction of flow orientation by the use of Laser–Doppler anemometry. An accompanying indirect calibration method needed for this scheme has also been developed based on the probability correlation between Doppler burst counts and the independently obtained mixture sample sizing number counts.

Results of measurements using this scheme have been presented for a laminar free stream flow and a turbulent shear flow of a dilute two-phase suspension of neutrally buoyant, spherical glass particles of distributed sizes in water. Reproducibility of these results has been confirmed.

Acknowledgement—This work has been done at the State University of New York at Stony Brook under Subcontract No. 360584-S for the Brookhaven National Laboratory of Contract No. A3014(03534) for the United States Nuclear Regulatory Commission. To these agencies, the authors would like to express their deep appreciation.

The authors also acknowledge Mr. Philip Pritchard for his contribution in the developing stages of this work.

REFERENCES

BEN-YOSEF, N., GINIO, O., MAHLAB, D. & WEITZ, A. 1975 Bubble size distribution measurement by Doppler velocimeter. *J. Appl. Phys.* **46**, 738–740.

DURST, F. & ELIASSON, B. 1975 Properties of Laser–Doppler signals and their exploitation for particle size measurements. *The Accuracy of Flow Measurements by Laser–Doppler Methods*, Proc. LDA-Symp., Copenhagen, 457–477.

DURST, F. & UMHAUER, H. 1975 Local measurements of particle velocities, size distribution and concentration with a combined Laser–Doppler particle sizing system. *The Accuracy of Flow Measurements by Laser–Doppler Methods*, Proc. LDA–Symp., Copenhagen, 430–456.

DURST, F. & ZARÉ, M. 1975 Laser–Doppler measurements in two-phase flows. *The Accuracy of Flow Measurements by Laser–Doppler Methods*, Proc. LDA-Symp., Copenhagen, 403–429.

EINAV, S. & LEE, S. L. 1973 Particles migration in laminar boundary layer flow. *Int. J. Multiphase Flow* **1**, 73–88.

FARMER, W. M. 1972 Dynamic particle size and number analysis using a Laser–Doppler velocity meter. *App. Optics* **11**, 2603.

GOLOVIN, V. A., KONYAEVA, N. P., RINKEVICHYUS, B. S. & YANINA, G. M. 1971 Study of the model of a two-phase flow using an optical quantum generator (Laser). UDC 541 · 12.012.

LEE, S. L. & EINAV, S. 1972 Migration in a laminar suspension boundary layer measured by the using of a two-dimensional Laser–Doppler Anemometer. *Progr. Heat Mass Transfer* **6**, 385–403.

MASON, J. S. & BIRCHENAUGH, A. 1975 The Application of Laser measurement techniques to the pneumatic transport of fine alumina particles. *Conference and Exhibition on the Engineering Uses of Coherent Optics*, Univ. of Strathclyde, Scotland.

MATTHES, W., RIEBOLD, W. & DECOOMAN, E. 1970 Measurement of the velocity of gas bubbles in water by a correlation method. *Rev. Scient. Instrum.* **41**, 843–845.

VAN DEHULST, H. C. 1957 *Light Scattering by Small Particles.* John Wiley, New York.